

Saturation of Electrical Resistivity in Metals at Large Temperatures

M. Calandra and O. Gunnarsson

Max-Planck-Institut für Festkörperforschung, D-70506 Stuttgart, Germany

(Received 20 June 2001; published 7 December 2001)

We present a microscopic model for systems showing resistivity saturation. An essentially exact quantum Monte Carlo calculation demonstrates that the model describes saturation. We give a simple explanation for saturation, using charge conservation and considering the limit where thermally excited phonons have destroyed the periodicity. Crucial model features are phonons coupling to the hopping matrix elements and a unit cell with several atoms. We demonstrate the difference to a model of alkali-doped C_{60} with coupling to the level positions, for which there is no saturation.

DOI: 10.1103/PhysRevLett.87.266601

PACS numbers: 72.10.Bg

In a metal, the electrical resistivity ρ grows with the temperature T due to the increased scattering of the electrons by phonons. Typically, $\rho(T) \sim T$ for large T . For some metals with a very large ρ , however, the resistivity saturates [1–3], i.e., it grows very slowly with T for large T . The resistivity is often described in a semiclassical (Boltzmann) picture, where an electron, on the average, travels a mean-free path l before it is scattered. The resistivity is inversely proportional to l . Typically, $l \gg d$, where d is the atomic separation. For systems with resistivity saturation, however, l becomes comparable to d . Work in the 1970s suggested that resistivity saturation occurs universally when $l \sim d$, the Ioffe-Regel condition [4], providing an upper limit to the large T resistivity of metals. Later work has, however, found exceptions, such as alkali-doped fullerenes [5,6].

Intuitively, resistivity saturation seems natural. One might expect that at the worst, an electron could be scattered at each atom, leading to $l \sim d$. Such a semiclassical picture, however, breaks down when $l \sim d$ [7], and it is contradicted by the lack of saturation for fullerenes. Several theories of the saturation have been presented, usually based on generalizations of the semiclassical Boltzmann theory, but none has been generally accepted [8–10].

The Bloch-Boltzmann theory starts from a periodic system and treats the scattering mechanisms as small perturbations. Here we consider the opposite limit, where thermally excited phonons have removed all effects of periodicity. In this limit, charge conservation naturally leads to saturation for systems with several atoms per unit cell and strong electron-phonon coupling, in particular for systems where the phonons couple to the hopping matrix elements. We show that this happens to occur when $l \sim d$. This does not happen, however, for a model of alkali-doped C_{60} , where the phonons couple to the level positions. We first use an essentially exact quantum Monte Carlo (QMC) calculation to demonstrate saturation in our model. We then introduce a method where the phonons are treated semiclassically and the electrons quantum mechanically, justifying the method by comparing with the QMC results. This method is sufficiently simple to allow for an interpretation of the results.

Saturation is clearly observed for, e.g., A15 compounds, such as Nb_3Sb [1], while Nb metal shows weak saturation at large T [11]. We study a model Nb_3^* of Nb_3Sb , where the Nb atoms have the same positions as in Nb_3Sb , but the Sb atoms are neglected [12]. This is compared with a model of Nb. We consider a cluster of N atoms, placed on A15 (Nb_3^*) or bcc (Nb) lattices with the lattice parameters 5.17 Å (Nb_3^*) or 3.28 Å (Nb).

We study the scattering of the electrons from phonons. Each atom is assumed to have vibrations in the three coordinate directions, described by Einstein phonons. The phonon energy, $\omega_{ph} = 14$ meV, is obtained from an average over the phonons of Nb [13]. For each Nb atom we include the fivefold degenerate ($n = 5$) d orbital. The hopping matrix elements between the orbitals are obtained from Harrison [14], using a power dependence on the atomic distance d ($\sim 1/d^m$). We use $m = 3.6$ more appropriate for Nb [15] than $m = 5$ used by Harrison. To avoid divergencies for very small d , $1/d^m$ is replaced by $1/(d^m + a^m)$, with $a = 2$ Å. The atomic vibrations modulate the hopping matrix elements, both due to the changes of the atomic distances and the relative movements of the orbital lobes. We neglect the influence of the vibrations on the level energies as well as the Coulomb interaction between the electrons. To obtain the resistivity, we calculate the current-current correlation function. The current operator \mathbf{j} is obtained by using charge and current conservation. Thus the matrix elements between orbitals ν and μ on sites \mathbf{R}^ν and \mathbf{R}^μ are

$$\mathbf{j}^{\nu\mu} = ie(\mathbf{R}^\nu - \mathbf{R}^\mu)t_{\nu\mu}, \quad (1)$$

where $t_{\nu\mu}$ are the corresponding hopping matrix elements.

This model can be solved essentially exactly by using a determinantal QMC method [16], treating the phonons quantum mechanically. For the models studied here, the QMC method has no “sign problem.” The calculated correlation function (for imaginary time) therefore has only (small) statistical errors. We use a maximum entropy method [17] to obtain the optical conductivity $\sigma(\omega)$ on the real frequency axis. The resistivity ρ is then $1/\sigma(0)$.

The left inset of Fig. 1 shows the QMC result (circles) for $\rho(T)$ of the Nb_3^* model. We are particularly interested in the large T behavior, which is also the limit where the QMC calculation can be performed with a reasonable effort. The large T result extrapolates to a substantial nonzero value. However, since the resistivity of the Nb_3^* model must go to zero for $T = 0$, the QMC calculation clearly shows that the model leads to a drastic reduction of the slope of the $\rho(T)$ curve for large T , usually referred to as resistivity saturation.

To analyze the results, we treat the phonons (semi)classically. The atomic displacements due to the phonons are chosen randomly according to a Gaussian distribution, determined from the average number of phonons at that temperature. For given “frozen” displacements, we calculate the hopping and current matrix elements. The eigenvalues ε_i and eigenvectors $|i\rangle$ of the resulting Hamiltonian are calculated. For an isotropic system, the optical conductivity is then given by

$$\sigma(\omega) \sim \frac{1}{\omega} \sum_{ij} |\langle i | j_x | j \rangle|^2 (f_i - f_j) \delta(\hbar\omega - \varepsilon_j + \varepsilon_i), \quad (2)$$

where f_i is the Fermi function for the state i .

The left inset of Fig. 1 shows that this approach (broken line) agrees quite well with the QMC calculation for large T , the temperature range we are interested in, and we expect the semiclassical calculation to remain accurate for $T \gg \omega_{\text{ph}}$ ($= 0.014$ eV). We can therefore interpret the results by analyzing the simpler semiclassical calculation. We observe that this model differs qualitatively from the (Ziman solution [18]) of the Boltzmann equation, in which $\rho(T) \sim T$ for large T . In the Boltzmann equation the

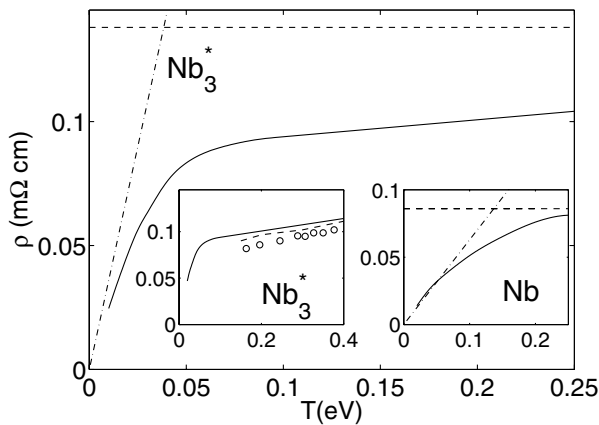


FIG. 1. Resistivity $\rho(T)$ as a function of temperature T . The main figure shows results for Nb_3^* ($N = 648$ atoms) and the right inset for Nb ($N = 640$ atoms). In both cases the phonons are treated semiclassically. The small T [Eq. (7)] (chain curves) and the large T [Eq. (5)] (broken curves) limits of $\rho(T)$ are also shown. The left inset compares the semiclassical [broken ($N = 36$) and full ($N = 648$) curves] and quantum Monte Carlo (circles, $N = 36$) calculations for Nb_3^* .

electrons are treated semiclassically, while here they are treated quantum mechanically.

Figure 1 shows that there is a very clear saturation for Nb_3^* , while for Nb (right inset) there is only weak saturation at large T , in agreement with experiment [1,11].

We now discuss this saturation. Figure 2a shows $\sigma(\omega)$ for Nb_3^* in the semiclassical theory. For small T , there is a narrow Drude peak at $\omega = 0$, which is smeared out for large T . Then $\sigma(\omega = 0)$ drops correspondingly. For $\omega > W$, $\sigma(\omega)$ remains zero (apart from a slight broadening introduced in the calculation), where W is the bandwidth, since there are no excitations for $\omega > W$.

The Drude peak is due to intraband transitions between states with similar values of the wave vector \mathbf{k} . As T is raised and the vibrations of the atoms are increased, the states lose their well-defined \mathbf{k} and band index labels. To illustrate this, we decompose a state $|i\rangle$ at a finite T in the $T = 0$ states with given \mathbf{k} vectors. The corresponding weights are labeled $c(i\mathbf{k})$. We define Δ as the average of $\Delta(i)$ over all states i , where

$$\Delta(i) = n_{\mathbf{k}} \sum_{\mathbf{k}} c(i\mathbf{k})^2, \quad (3)$$

and $n_{\mathbf{k}} = 256$ is the number of allowed \mathbf{k} vectors for the systems studied. If each state has $n_{\mathbf{k}}/m$ \mathbf{k} components with equal weights, $\Delta = m$. If periodicity is completely lost, $\Delta = 1$, and if each state has only one \mathbf{k} component, $\Delta = n_{\mathbf{k}}$ ($= 256$) [19]. Δ is shown in Fig. 3. It illustrates how the effects of periodicity are lost very quickly for Nb_3^* on a temperature scale of just a few hundred K.

For a large T , the ($\mathbf{q} \rightarrow \mathbf{0}$) current operator then couples all states to each other. We now make the assumption that at large T the coupling between all states is equally strong [20]. This is the opposite limit to the Boltzmann treatment, where \mathbf{k} is assumed to be a good quantum number. We replace a current matrix element in Eq. (2) by

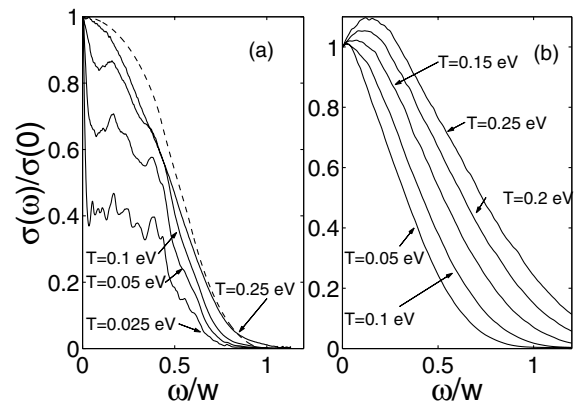


FIG. 2. Optical conductivity as a function of frequency ω for the (a) A15 and (b) fullerene models in the semiclassical calculation. The frequency has been scaled by the $T = 0$ bandwidth W . (a) also shows (broken curve) the result of approximating all current matrix elements by their average.

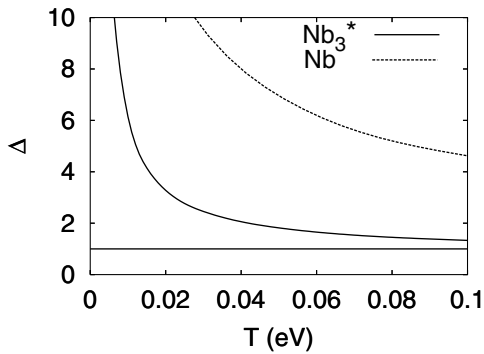


FIG. 3. The measure Δ [Eq. (3)] of the amount of momentum conservation as a function of T for Nb_3^* (full line) and Nb (broken line). The horizontal line represents a complete loss of momentum conservation.

its average $|j_x^{\text{av}}|^2$ over all transitions. Using charge and current conservation [Eq. (1)], we obtain

$$|j_x^{\text{av}}|^2 = \frac{e^2 d^2}{3N^2 n^2} \sum_{\nu\mu} |t_{\nu\mu}|^2 = \frac{e^2 d^2}{3Nn^2} \langle \varepsilon^2 \rangle, \quad (4)$$

where n is the orbital degeneracy, $\langle \varepsilon^2 \rangle$ is the second moment of the density of states $N(\varepsilon)$ per atom, and d is a typical atomic separation. We assume some generic shape of $N(\varepsilon)$. Since we know its second moment, we can then relate $N(\varepsilon)$ to the j_x^{av} . Using this relation, we can calculate $\sigma(\omega)$, shown by the broken curve in Fig. 2a. A comparison with the full calculation shows that this approximation becomes rather accurate already at a moderate T . We find that $\sigma(0) \sim d^2/\Omega$, where Ω is the volume per atom. Using the $T = 0$ nearest neighbor distance for d , we obtain

$$\rho \sim A \frac{d}{n}. \quad (5)$$

A depends on the precise assumptions of the model, but it is $\sim 0.2 \text{ m}\Omega\text{cm}$ if d is expressed in \AA . Assuming a semielliptical density of states $\sim \sqrt{(W/2)^2 - \varepsilon^2}$ and band filling 0.4, we find $A = 0.27$ and $0.15 \text{ m}\Omega\text{cm}$ for the A15 and bcc lattices, respectively. This is shown by the broken horizontal lines in Fig. 1. Given the simple assumptions, the agreement with the full semiclassical calculations at large T is surprisingly good. The corresponding apparent mean-free path is

$$l \sim cn^{1/3}d. \quad (6)$$

With the assumptions above, we obtain $c = 0.5$ and $c = 0.6$ for the A15 and bcc lattices, respectively. Saturation therefore happens roughly when the Ioffe-Regel condition is satisfied, as might have been expected on dimensional grounds.

The derivation of Eq. (6) uses a quantum-mechanical treatment of the electrons. It explains why metals with a large resistivity usually show saturation, and why it happens when $l \sim d$.

The $\rho(T)$ in Eq. (5) is independent of T , while Fig. 1 shows a weak T dependence, even after saturation. This

is partly due to the T dependence of the Fermi functions in Eq. (2), which were approximated by θ functions in the derivation above. There is also a T dependence due to changes of the *shape* of the density of states as T is increased, which was neglected above by using a “generic” density of states. These effects are important only when T is an appreciable fraction of the bandwidth (for realistic values of the electron-phonon coupling).

Equations (5) and (6) are obtained by assuming that the Drude peak has been smeared out and that $\sigma(\omega)$ is spread out over the whole bandwidth. Both the saturation resistivity and the corresponding mean-free path are independent of the bandwidth. A scaling of $t_{\nu\mu}$ by a factor $\alpha > 1$ increases W , and $\sigma(\omega)$ extends over a larger energy range. At the same time, however, j_x^{av} is increased [Eq. (1)] in such a way that $\sigma(0)$ in Eq. (2) is unchanged. Charge and current conservation therefore plays a crucial role for our results (5), (6).

We next consider a small T ($> \omega_{\text{ph}}$). Then [18]

$$\rho(T) = 8\pi^2 \frac{\lambda T k_B}{\hbar \Omega_{\text{pl}}^2}, \quad (7)$$

where λ is the electron-phonon coupling constant and k_B is the Boltzmann constant. Ω_{pl} is the plasma frequency

$$(\hbar \Omega_{\text{pl}})^2 = \frac{e^2}{3\pi^2} \sum_n \int_{Bz} d^3k \left[\frac{\partial \varepsilon_{n\mathbf{k}}}{\partial \mathbf{k}} \right]^2 \delta(\varepsilon_{n\mathbf{k}} - E_F), \quad (8)$$

where $\varepsilon_{n\mathbf{k}}$ is the energy of a state with the band index n and the wave vector \mathbf{k} and E_F is the Fermi energy. Ω_{pl} depends on the average Fermi velocity.

The straight line given by Eq. (7) (chain lines in Fig. 1), agrees well with the semiclassical calculations for small T . Typically, this line rises so slowly that it intersects the horizontal line of Eq. (5) well above the melting point for the metal of interest. Then no saturation is found in the accessible temperature range. If, however, Ω_{pl} is small and λ is large, the two lines cross below the melting temperature. Saturation is then observed. An important difference between Nb_3^* and Nb is that Nb_3^* has many rather flat bands, due to the large unit cell [8] and many forbidden crossings. The resulting small electron velocities lead to a small Ω_{pl} . We find $\Omega_{\text{pl}} = 3.6$ and 8.2 eV for Nb_3^* and Nb , respectively, which makes the slope of the line in Eq. (7) about a factor of 5 larger for Nb_3^* than for Nb . We find similar λ 's for Nb_3^* ($\lambda = 1.0$) and Nb ($\lambda = 0.9$). More accurate estimates give $\Omega_{\text{pl}} = 3.4 \text{ eV}$ (Nb_3Sn) [21] and 9.5 eV (Nb) [22] and $\lambda = 1.7$ (Nb_3Sn) [3] and 1.1 (Nb) [22].

It is interesting to replace the d orbitals in our Nb_3^* model by s orbitals. As before, the resistivity shows saturation, but the saturation is less pronounced than in Fig. 1. The saturation resistivity [Eq. (5)] is larger due to the smaller degeneracy ($n = 1$).

A very different behavior is found in the alkali-doped fullerenes [A_3C_{60} ($\text{A} = \text{K}, \text{Rb}$)], where the apparent

mean-free path becomes much shorter than the separations of the C_{60} molecules [5,6]. This behavior was related to the fact that the important (intramolecular) phonons primarily couple to the C_{60} level energies, instead of the hopping matrix elements [23,24]. Already at a moderate T , the resulting fluctuations in the level energies become comparable to the $T = 0$ width of the narrow t_{1u} band, which conducts the current. This leads to a broadening of the t_{1u} band and of $\sigma(\omega)$ beyond the $T = 0$ bandwidth. In contrast to the case of a scaling of the hopping parameters, discussed below Eq. (6), this is, however, not accompanied by an increase of the current operator. Thus $\sigma(0)$ is reduced, explaining the lack of saturation. This is illustrated in Fig. 2b.

It is interesting to compare the cases when the phonons couple to the level energies (LE coupling) and to the hopping integrals (HI coupling). We have studied the case of HI coupling in a C_{60} model. By assuming an unrealistically small phonon frequency for the intermolecular vibrations, we can obtain the same value of λ as for the LE coupling. For the HI coupling, we then find that the resistivity of our C_{60} model shows saturation. We have also considered LE coupling in the Nb_3^* model. The resulting resistivity shows a change in slope, somewhat similar to Fig. 1, but with a larger slope for large T than in Fig. 1. These results illustrate that it is possible to obtain saturation with LE coupling, but that HI coupling is more appropriate for describing saturation.

Our semiclassical treatment of the two models is closely related to conduction in disordered systems with diagonal (DD) or (ODD) off-diagonal disorder. While DD models can give localization, no localization was found close to the center of the band in a ODD model [26]. This is consistent with the saturation seen in Fig. 1 for the A15 model, having ODD in the semiclassical treatment. For the C_{60} model, the semiclassical treatment gives localization for a large DD. The QMC treatment, however, takes into account that the disorder is not static but due to thermal fluctuations and that the scattering can be inelastic. In this QMC treatment we find a lack of saturation, but we have not seen signs of localization.

To summarize, guided by the loss of periodicity at large T , we have studied the effect of replacing the current matrix element by its average. Together with charge conservation, this leads to clear saturation in a model where the phonons couple to the hopping matrix elements. On the other hand, saturation does not happen in a model for A_3C_{60} , where the phonons couple to the level energies. The issue of saturation or not saturation is raised only for experimentally accessible temperatures if λ is large and Ω_{pl} is small. This is favored by the relatively flat bands for Nb_3^* (Ω_{pl} small) and by the small bandwidth for A_3C_{60} (λ large and Ω_{pl} small).

We would like to thank M. Föhnle, O. Jepsen, E. Koch, and R. Zeyher for useful discussions, M. Jarrell for making his MaxEnt program available, and the Max-Planck-Forschungspreis for financial support.

-
- [1] Z. Fisk and G. W. Webb, Phys. Rev. Lett. **36**, 1084 (1976).
 - [2] Z. Fisk and A. C. Lawson, Solid State Commun. **13**, 277 (1973).
 - [3] P. B. Allen, in *Superconductivity in d- and f-Band Metals*, edited by H. Suhl and M. B. Maple (Academic, New York, 1980), p. 291.
 - [4] A. F. Ioffe and A. R. Regel, Prog. Semicond. **4**, 237 (1960).
 - [5] A. F. Hebard *et al.*, Phys. Rev. B **48**, 9945 (1993).
 - [6] J. H. Schön, Ch. Kloc, and B. Batlogg, Nature (London) **408**, 549 (2000).
 - [7] W. Kohn and J. M. Luttinger, Phys. Rev. **108**, 590 (1957).
 - [8] B. Chakraborty and P. B. Allen, Phys. Rev. Lett. **42**, 736 (1979).
 - [9] P. J. Cote and L. V. Meisel, Phys. Rev. Lett. **40**, 1586 (1978).
 - [10] A. Ron, B. Shapiro, and M. Weger, Philos. Mag. B **54**, 553 (1986).
 - [11] J. M. Abraham and B. Deviot, J. Less-Common Met. **29**, 311 (1972).
 - [12] W. E. Pickett, K. M. Ho, and M. L. Cohen, Phys. Rev. B **19**, 1734 (1979).
 - [13] E. L. Wolf, *Principles of Electron Tunnelling Spectroscopy* (Oxford University Press, New York, 1985), p. 268.
 - [14] W. Harrison, *Electronic Structure and the Properties of Solids: The Physics of the Chemical Bond* (Dover, New York, 1980).
 - [15] O. Jepsen (private communication).
 - [16] R. Blankenbecler, D. J. Scalapino, and R. L. Sugar, Phys. Rev. D **24**, 2278 (1981).
 - [17] M. Jarrell and J. E. Gubernatis, Phys. Rep. **269**, 133 (1996).
 - [18] G. Grimvall, *The Electron-Phonon Interaction in Metals* (North-Holland, Amsterdam, 1981), p. 212; *ibid.*, p. 216.
 - [19] For $T \approx 0$, $\Delta \approx 0.1n_k < n_k$ for the clusters considered in Fig. 3, due to mixing of degenerate \mathbf{k} states.
 - [20] The matrix elements of the current operator have a broad distribution of values. However, an average over states with the similar energies, appropriate in Eq. (2), has fairly small variations already at moderate T .
 - [21] L. F. Mattheiss and L. R. Testardi, Phys. Rev. B **17**, 4640 (1978).
 - [22] S. Y. Savrasov and D. Y. Savrasov, Phys. Rev. B **54**, 16487 (1996).
 - [23] O. Gunnarsson and J. E. Han, Nature (London) **405**, 1027 (2000).
 - [24] A similar model was used to describe resistivity saturation [25]. We find, however, that this model is more appropriate for describing the lack of saturation.
 - [25] A. J. Millis, J. Hu, and S. Das Sarma, Phys. Rev. Lett. **82**, 2354 (1999).
 - [26] P. D. Antoniou and E. N. Economou, Phys. Rev. B **16**, 3768 (1977).